



THE UNIVERSITY *of* EDINBURGH

Edinburgh Research Explorer

Evidence that Fetal Death is Associated with Placental Aging

Citation for published version:

Maiti, K, Sultana, Z, Aitken, RJ, Morris, J, Park, F, Andrew, B, Riley, SC & Smith, R 2017, 'Evidence that Fetal Death is Associated with Placental Aging', *American Journal of Obstetrics & Gynecology (AJOG)*.
<https://doi.org/10.1016/j.ajog.2017.06.015>

Digital Object Identifier (DOI):

[10.1016/j.ajog.2017.06.015](https://doi.org/10.1016/j.ajog.2017.06.015)

Link:

[Link to publication record in Edinburgh Research Explorer](#)

Document Version:

Version created as part of publication process; publisher's layout; not normally made publicly available

Published In:

American Journal of Obstetrics & Gynecology (AJOG)

General rights

Copyright for the publications made accessible via the Edinburgh Research Explorer is retained by the author(s) and / or other copyright owners and it is a condition of accessing these publications that users recognise and abide by the legal requirements associated with these rights.

Take down policy

The University of Edinburgh has made every reasonable effort to ensure that Edinburgh Research Explorer content complies with UK legislation. If you believe that the public display of this file breaches copyright please contact openaccess@ed.ac.uk providing details, and we will remove access to the work immediately and investigate your claim.



Accepted Manuscript

Evidence that Fetal Death is Associated with Placental Aging

Kaushik Maiti, Zakia Sultana, Robert John Aitken, Jonathan Morris, Felicity Park, Bronwyn Andrew, Simon C. Riley, Roger Smith



PII: S0002-9378(17)30756-1

DOI: [10.1016/j.ajog.2017.06.015](https://doi.org/10.1016/j.ajog.2017.06.015)

Reference: YMOB 11732

To appear in: *American Journal of Obstetrics and Gynecology*

Received Date: 1 May 2017

Revised Date: 6 June 2017

Accepted Date: 13 June 2017

Please cite this article as: Maiti K, Sultana Z, Aitken RJ, Morris J, Park F, Andrew B, Riley SC, Smith R, Evidence that Fetal Death is Associated with Placental Aging, *American Journal of Obstetrics and Gynecology* (2017), doi: 10.1016/j.ajog.2017.06.015.

This is a PDF file of an unedited manuscript that has been accepted for publication. As a service to our customers we are providing this early version of the manuscript. The manuscript will undergo copyediting, typesetting, and review of the resulting proof before it is published in its final form. Please note that during the production process errors may be discovered which could affect the content, and all legal disclaimers that apply to the journal pertain.

Title: Evidence that Fetal Death is Associated with Placental Aging

Authors: Kaushik MAITI^{1,2}, Zakia SULTANA^{1,2}, Robert John AITKEN², Jonathan MORRIS³, Felicity PARK⁴, Bronwyn ANDREW⁴, Simon C. RILEY⁵ and Roger SMITH^{*1, 2}

Affiliations:

¹Mothers and Babies Research Centre, Hunter Medical Research Institute, Lot 1 Kookaburra Circuit, New Lambton Heights, NSW 2305, Australia

²Priority Research Centre in Reproductive Science, Faculty of Health, University of Newcastle, Callaghan, NSW 2308, Australia

³Kolling Institute, Royal North Shore Hospital, University of Sydney, NSW 2065, Australia

⁴Department of Obstetrics and Gynaecology, John Hunter Hospital, New Lambton Heights, NSW 2305, Australia

⁵MRC Centre for Reproductive Health, University of Edinburgh, Edinburgh, EH16 4TJ, UK

Disclosure Statement: KM and RS hold patents through the University of Newcastle on AOX1 as a therapeutic target and the use of placental aging related markers as diagnostics to predict stillbirth.

Funding: The study was funded by John Hunter Hospital Charitable Trust Grant 2013 (G1300740), Stillbirth Foundation Australia Grant 2014 (G1400089), Haggarty Foundation and NH&MRC grant (APP1084782).

***Corresponding Author:**

Laureate Professor Roger Smith AM

Mothers and Babies Research Centre, Hunter Medical Research Institute, Lot 1 Kookaburra Circuit, New Lambton Heights, NSW 2305, Australia

Email: roger.smith@newcastle.edu.au

Phone Number: 61-2-49214380, **Fax Number:** 61-2-49214394

26 **Word Count:** 320 (Abstract), 3,933 (Main Text).

ACCEPTED MANUSCRIPT

27 **Condensation:**

28 Fetal death is associated with features of placental aging.

29

30 **Short title:** Fetal Death and Placental Aging

31

32

Abstract**Background:**

The risk of unexplained fetal death or stillbirth increases late in pregnancy suggesting that placental aging is an etiological factor. Aging is associated with oxidative damage to DNA, RNA and lipids. We hypothesized that placentas at more than 41 completed weeks of gestation (late-term) would show changes consistent with aging that would also be present in placentas associated with stillbirths.

Objective:

We sought to determine whether placentas from late-term pregnancies and unexplained stillbirth show oxidative damage and other biochemical signs of aging. We also aimed to develop an *in vitro* term placental explant culture model to test the aging pathways.

Study design:

We collected placentas from women at 37-39 weeks gestation (early-term and term), late-term and with unexplained stillbirth. We used immunohistochemistry to compare the three groups for: DNA/RNA oxidation (8-hydroxy-deoxyguanosine, 8OHdG), lysosomal distribution (Lysosome-associated membrane protein 2, LAMP2), lipid oxidation (4-hydroxynonenal, 4HNE), and autophagosome size (Microtubule-associated proteins 1A/1B light chain 3B, LC3B). The expression of aldehyde oxidase 1 (AOX1) was measured by real-time PCR. Using a placental explant culture model, we tested the hypothesis that AOX1 mediates oxidative damage to lipids in the placenta.

Results:

Placentas from late-term pregnancies show increased AOX1 expression, oxidation of DNA/RNA and lipid, perinuclear location of lysosomes and larger autophagosomes compared to placentas from women delivered at 37-39 weeks. Stillbirth associated placentas showed similar changes in oxidation of DNA/RNA and lipid, lysosomal location and autophagosome

size to placentas from late-term. Placental explants from term deliveries cultured in serum free medium also showed evidence of oxidation of lipid, perinuclear lysosomes and larger autophagosomes, changes that were blocked by the G protein-coupled estrogen receptor 1 (GPER1) agonist G1, while the oxidation of lipid was blocked by the AOX1 inhibitor raloxifene.

Conclusions:

Our data are consistent with a role for AOX1 and GPER1 in mediating aging of the placenta that may contribute to stillbirth. The placenta is a tractable model of aging in human tissue.

Key words: placenta; aging; stillbirth; fetal death; autophagosome; DNA / RNA oxidation; lipid oxidation; AOX1; GPER1; raloxifene; placental explant culture

Glossary of Terms

Aldehyde Oxidase 1(AOX1) — an oxidizing enzyme with a wide range of substrates, that generates peroxides

Autophagosome — an intracellular organelle that collects damaged proteins and old mitochondria

G protein-coupled estrogen receptor 1 (GPER1) — a cell surface estrogen receptor distinct from nuclear estrogen receptors

8-hydroxy-deoxyguanosine (8OHdG) — a product of DNA oxidation

4-hydroxynonenal (4HNE) — a product of lipid peroxidation

Lipid peroxidation — the oxidative degradation of lipids

Lysosome — an intracellular organelle that contains proteolytic enzymes in an acid environment

Introduction

Unexplained fetal death is a common complication of pregnancy occurring in approximately 1 in 200 pregnancies in developed countries¹ and more frequently in the developing world. While no cause has been established, the rate of fetal death rises rapidly as gestation progresses beyond 38 weeks². Johnson *et al.*³ have proposed the operational definition of aging as an increase in risk of mortality with time, which is consistent with a role for aging in the etiology of stillbirth⁴. Supporting this view a histopathological study of placentas associated with cases of unexplained intrauterine death at term revealed that 91% showed thickening of the maternal spiral artery walls, 54% contained placental infarcts, 10% had calcified areas and 13% demonstrated vascular occlusion⁵, another reported increased atherosclerosis⁶; changes that are associated with aging in other organs. Supporting a link between placental aging and stillbirth, Ferrari *et al.*, have recently reported that telomere length is reduced in placentas associated with stillbirth⁷. Fetal growth restriction is also associated with both stillbirth and telomere shortening⁸. We therefore sought to determine whether placentas from women who delivered after 41 completed weeks (late-term) or had stillbirth had biochemical evidence of aging. As markers of aging we chose to measure 8-hydroxy-deoxyguanosine (a marker of DNA oxidation) and 4-hydroxynonenal (a marker of lipid oxidation) as both have been described to increase in the brain with aging, and the enzyme aldehyde oxidase which is known to generate oxidative damage in the kidney. Aging is also known to affect the effectiveness of the intracellular recycling process that involves fusion of acidic hydrolase containing lysosomes with autophagosomes, we therefore sought changes in these intracellular organelles in the late-term placentas and those associated with stillbirth.

Materials and Methods

Ethics, Collection and Processing of Tissues

This study was approved by the human research ethics committee of the Hunter New England Health Services and the University of Newcastle, NSW, Australia. Human placentas were collected after written informed consent was obtained from the patients by midwives. Placentas were collected from women at 37-39 weeks gestation undergoing caesarean section for previous caesarean section or normal vaginal delivery, women at 41⁺ weeks gestation undergoing caesarean section or normal vaginal delivery, and women who had stillborn infants undergoing vaginal delivery. Placentas were collected immediately after delivery and processed without further delay. Villous tissues were sampled from multiple sites and prepared for histology and RNA extraction. For each placenta, tissues were obtained from at least 5 different regions of the placenta and 4-5 mm beneath the chorionic plate. Samples from each individual placenta were immediately frozen under liquid nitrogen and stored at -80° C until subsequent experiments. For histology experiments, tissues were fixed in 2% formaldehyde for 24 h, stored in 50% ethanol at room temperature (RT) and embedded in paraffin. To create a placental roll a 2 cm strip of chorioamniotic membrane was cut from the periphery of the placenta keeping a small amount of placenta attached to the membrane. The strip was rolled around forceps leaving residual placenta at the centre of the cylindrical roll. The cylindrical roll was then cut perpendicular to the cylindrical axis to obtain 4 mm thick sections and fixed in formalin. Placentas from patients with infection, diabetes, pre-eclampsia, placenta praevia, intra-uterine growth restriction or abruption were excluded.

Reagents and Antibodies

Antibodies against LAMP2 and AOX1 were obtained from BD Biosciences (North Ryde, Australia) and Proteintech (Rosemont, USA), respectively. Antibody against LC3B and GPER1 were obtained from Novus Biologicals (Littleton, USA). Antibodies against 8OHdG

and 4HNE were purchased from Abcam (Melbourne, Australia). Dulbecco's modified Eagle's medium (DMEM), antibiotic-antimycotic (anti-anti), Nupage precast 12 well protein gel and prolong gold antifade mounting media with DAPI, Alexa conjugated secondary antibodies were obtained from Thermo Fisher Scientific Australia Pty (Scoresby, Australia). The horse radish peroxidase (HRP) conjugated secondary antibodies were purchased from Cell Signalling Technologies (Beverly, MA, USA). Fetal bovine serum was obtained from Bovogen Biologicals Pty Ltd (VIC, Australia). Protease inhibitor and phosphatase inhibitor were supplied by Roche (Castle Hill, Australia). Raloxifene was purchased from Sigma-Aldrich (Sydney, Australia) and G1 was supplied by Tocris-bioscience (Bristol, UK). The BCA protein assay kit was obtained from Thermo Fisher Scientific (Scoresby, Australia). All other chemicals were purchased from either Ajax Finechem Pty Ltd or Sigma-Aldrich (Sydney, Australia).

Placental Explant Culture

For *in vitro* experiments, human term placentas (all at 39 weeks of gestation) were obtained from women with normal singleton pregnancies without any symptoms of labour after an elective (a scheduled repeat) caesarean section. Placentas were collected immediately after delivery and prepared for explant culture. Villous tissues of placentas were randomly sampled from different regions of the placenta 4-5 mm beneath the chorionic plate. Tissues were washed several times with Dulbecco's phosphate-buffered saline (PBS) under sterile conditions to remove excess blood. Villous explants of $\sim 2 \text{ mm}^3$ were dissected and placed into 100 mm culture dishes (30 pieces/dish) containing 25 ml of DMEM supplemented with 2 mM L-glutamine, 1% Na-pyruvate, 1% penicillin/streptomycin (100X) solution with the addition of 10% (v/v) fetal bovine serum (FBS) and cultured in a cell culture chamber at 37 °C temperature under 95% air (20% oxygen) and 5% CO₂ for 24 h. At day 2, villous explants

were transferred to fresh 30 ml growth medium and incubated in a cell culture chamber for 90 minutes and washed in DMEM without FBS (referred to as 'serum-free medium' or 'growth factor deficient medium'). Next 6-7 pieces of villous tissue weighing approximately 400 mg were transferred to a culture dish (60 mm) containing 6 ml serum-free medium with or without the addition of pharmacological agents, for example, raloxifene (1 nM) or the GPER1 agonist G1 (1 nM), for subsequent incubation for 24 h. At the end of 24 h some tissues were fixed in 2% formaldehyde, subjected to routine histological processing and embedded in paraffin wax, and some tissues were immediately frozen in liquid nitrogen and stored at -80 °C until subsequent experiments. For each placental explant culture, samples were also collected at time '0 (zero)' h i.e., before incubation in serum free medium, and were formalin fixed and stored frozen at -80 °C until further experiments.

Western Blotting

The western blotting was performed as previously described⁹. Samples of placenta (1gm) were crushed under liquid nitrogen. Aliquots of 100 mg of placental tissues were homogenised in 1 ml of lysis buffer (PBS, 1% Triton-X-100, 0.1 % Brij-35, 1 X protease inhibitor, 1 X phosphatase inhibitor, pH 7.4). The protein concentration of each placental extract was measured using a BCA protein assay kit and 40 µg of placental extract was separated by electrophoresis in NuPage bis-tris precast 12 well gels for 50 mins at a constant 200 V. Separated proteins were then transferred to nitrocellulose membrane using a Novex transfer system for 70 mins and blocked overnight at 4 °C with 1% bovine serum albumin (BSA) in tris buffered saline with 0.1 % tween-20 (TBST). The membranes were then incubated with primary antibody in 1% BSA in TBST for 2 hours at RT, then washed three times with TBST, followed by incubating with HRP conjugated secondary antibodies in 1% BSA in TBST for an hour. After three further washes with TBST, the immuno-reactive bands

were developed in Luminata reagent (Merck Millipore) and detected using an Intelligent Dark Box LAS-3000 Imager (Fuji Photo Film, Tokyo, Japan).

Immunohistochemistry

Fluorescent immunohistochemistry (IHC) was performed according to previously published methods⁹. Six μ m paraffin placental sections were deparaffinised and hydrated, then heated with tris-EDTA buffer (pH 9) in a microwave oven for antigen retrieval. The sections were blocked with 1 % BSA in TBST for an hour at RT. The sections were incubated with primary antibodies overnight and washed three times with TBST, before incubation with Alexa-conjugated secondary antibodies for 90 mins. The sections were mounted with prolong gold antifade mounting media with DAPI. The fluorescent photographs for Figures 2, 3, 4, 5, 6, 7, S1, S2 and S3 were taken on a Nikon eclipse 90i confocal microscope (Nikon Instruments Inc.). The fluorescent photographs for Figure 8 were taken on Nikon eclipse Ti fluorescence microscope (Nikon Instruments Inc.).

RNA isolation and Real time PCR

Placental tissues were crushed under liquid nitrogen. Approximately 100 mg of crushed placental tissues were homogenised in 2 ml of Trizol reagent (Life Technologies) with an Ultra Turrax homogenizer. Total RNA was extracted from the Trizol-extract by Direct-zol™ RNA MiniPrep (Zymo Research). The RNA was treated with DNase and purified with a RNA Clean & Concentrator™-5 kit (Zymo Research). The RNA quality was checked by running the DNase treated sample in agarose gel with ethidium bromide in 1X TAE buffer. The purified RNA was used to make cDNA using a SuperScript® III First-Strand Synthesis System kit (Life Technologies). The cDNA was used to run real time PCR by Taqman primers for aldehyde oxidase 1 (AOX1) (Life Technologies, Assay ID: Hs00154079_m1) and

Taqman gene expression master mix (Life Technologies) with an internal control of 18s ribosomal RNA (Life Technologies) to quantify mRNA for AOX1. We used a SyBr green master mix to quantify mRNA for G-protein coupled receptor 1 (GPER1) (Invitrogen, Forward primer 5'-CGTCCTGTGCACCTTCATGT-3' Backward primer 5'-AGCTCATCCAGGTGAGGAAGAA-3') with respect to beta-actin as an internal control using an Applied Biosystem 7500 PCR system.

Statistical analysis

Sample numbers are shown in the legends to individual figures. The data in Figures 2, 4, 5, 6 and 8 were analysed using the Mann-Whitney test (two way) and results are presented as scatter plots showing the median. The data in Figure 7, S2 and S3 were analysed using the Wilcoxon matched-pairs signed rank test and results are presented as mean showing the standard error of the mean (S.E.M.). All the *p*-values were calculated using the Graphpad Prism software (Version 7, Graph Pad Software Inc., San Diego, California). A *p*-value of ≤ 0.05 was considered statistically significant.

Results

Subject characteristics

Demographic and clinical characteristics of the study participants are reported in table 1.

Relationship between stillbirth risk and length of gestation

To illustrate the relationship between stillbirth risk and length of gestation we created a Kaplan Myer plot of the data on human gestational length in a population with relatively low levels of medical intervention from Omigbodun and Adewuyi¹⁰ and combined it with the data on risk of stillbirth per 1000 continuing pregnancies from Sutan *et al.*² (Figure 1 reproduced

with permission⁴). The data illustrate that stillbirth is consistent with an aging etiology as defined by Johnson *et al.*³.

DNA/RNA Oxidation

We sought evidence of placental DNA/RNA oxidation as measured by 8-hydroxy-deoxyguanosine (8OHdG), as a marker of DNA/RNA oxidation that has previously been observed in aging tissues¹¹ such as the brain in Alzheimer's disease¹². Immunohistochemistry (IHC) was performed for 8OHdG and the average intensity of 8OHdG staining in nuclei/frame demonstrated a significant increase in DNA/RNA oxidation in late-term and stillbirth associated placentas (Figure 2).

Movement and clustering of lysosomes in late-term and stillbirth placentas

Misfolded proteins and damaged mitochondria are normally recycled in autophagosomes in a process that involves autophagosome fusion with proteolytic enzyme containing lysosomes. Accumulation of abnormal protein is thought to play a role in aging particularly in the brain, for instance the accumulation of tau and amyloid protein in Alzheimer's disease^{13, 14} and mutant huntingtin in Huntington's disease¹⁵. In Huntington's disease, the distribution of the lysosomes within neurones is altered with increased perinuclear accumulation of lysosomes¹⁶. We used a lysosomal marker, lysosome-associated membrane protein-2 (LAMP2) to analyse the distribution of lysosomes in the placenta by IHC. IHC showed lysosomes positioned on the apical surface of early-term placental syncytiotrophoblast (Figures 3A, 3D and 3E), whereas lysosomes relocated to the perinuclear and the basal surface in late-term and stillbirth placentas (Figures 3B, 3C, 3F and 3G).

Lipid oxidation in placental tissue

The increase in DNA oxidation which we had demonstrated suggested free radical damage that might also lead to lipid peroxidation. Lipid peroxidation has been observed to increase in Alzheimer's disease as measured by the formation of 4-hydroxynonenal (4HNE)¹⁷. We therefore performed IHC for 4HNE in late-term, stillbirth and 37-39 weeks placental tissue. This revealed a marked, statistically significant increase in 4HNE staining in late-term syncytiotrophoblast that we also observed in placentas associated with stillbirth shown in Figure 4 (A-D).

Larger autophagosomes containing 4HNE occur in late-term and stillbirth associated placentas

Inhibition of autophagosome function with failure of fusion with lysosomes leads to an increase in autophagosome size^{18, 19}. This process leads to inhibition of overall autophagic function that is seen in Alzheimer's disease¹⁸, Danon's disease¹⁹ and neurodegeneration²⁰. We detected autophagosomes using IHC with an antibody against LC3B. We observed a significant increase in the size of autophagosomes (Figure 5D) in both late-term (Figure 5B) and stillbirth (Figure 5C) associated placentas compared to 37-39 week placentas (Figure 5A). Dual labelled fluorescence immunostaining showed that the larger autophagosomes of late-term and stillbirth placentas contained 4HNE, a product of lipid peroxidation (Supplementary Figure S1).

Role of aldehyde oxidase 1 (AOX1) in placental oxidative damage

Aldehyde oxidase 1 (AOX1) is a molybdoflavoenzyme, which oxidises a range of aldehydes including 4HNE into corresponding acids and peroxides²¹. We provide evidence that AOX1 is involved in the generation of the increased 4HNE observed in late-term and stillbirth associated placentas using co-localisation. Dual labelled fluorescence IHC showed that AOX1

co-localises to 4HNE positive particles in late-term (Figure 6A-C) and stillbirth placentas (Figure 6D-F). Additionally real-time qPCR showed that late-term and stillbirth placentas expressed significantly higher mRNA for AOX1 than 37-39 week placentas (6G). These data support the concept that AOX1 plays a role in the oxidative damage that occurs in the late-term and stillbirth associated placentas.

Pharmacological inhibition of AOX1 using placental explant culture

Our data provide clear evidence for increased lipid oxidation, disordered lysosome-autophagosome interactions and increased AOX1 expression in the late-term and stillbirth placental syncytiotrophoblast. To determine if these events were causally linked we developed a placental explant culture system using term placental tissue cultured in serum-free (growth factor deficient) medium. IHC showed that serum deprivation significantly increased production of 4HNE at 24 h after incubation (Figure 7A-C, F and G). We also found a significant increase in the size of autophagosomes (Supplementary Figure S2) and a change in lysosomal distribution to a perinuclear location after 24 h incubation in serum-free medium (Supplementary Figure S3). We sought to determine cause and effect relationships between the development of lipid oxidation observed when placental explants were cultured in the absence of serum, and AOX1. To achieve this we used a potent AOX1 inhibitor, raloxifene²² and a GPER1 agonist, G1. We used the GPER1 agonist G1 as we had detected GPER1 expression on the apical surface of syncytiotrophoblast (Figure 8A and B) and the GPER1 agonist has been shown to inhibit production of 4HNE in the kidney²³. Both raloxifene and G1 inhibited the production of 4HNE in the serum starved placental explants after 24 h of treatment (Figure 7D, E, F and G). G1 also prevented the changes in lysosomal distribution within the syncytiotrophoblast (Supplementary Figure S3).

Presence of the cell surface estrogen receptor GPER1 on the apical surface of the syncytiotrophoblast

As the GPER1 agonist had evident effects in placental explant cultures we undertook characterisation of GPER1 expression in placental tissue. The expression of GPER1 in a section of placenta roll (described in the Method section) detected by fluorescent IHC showed that GPER1 is expressed in placental villi (Figure 8A), which at higher magnification (100X), was localised to the apical surface of placental villi (Figure 8B). Real time PCR for GPER1 showed that placental villi have significantly higher expression of GPER1 than amnion, chorion or decidua (Figure 8C). Western-blot for GPER1 also confirmed higher protein levels of GPER1 in placental villous tissue than amnion, chorion or decidua (Figure 8D). The demonstration of GPER1 localisation on the apical surface of the syncytiotrophoblast indicates the plausibility of estrogen inhibition of AOX1 activity in the placenta.

Comment

Our data indicate that between 37-39 and 41 weeks of gestation dramatic changes occur in the biochemistry and physiology of the placenta. In particular there is increased oxidative damage to DNA/RNA and lipid, a change in position of lysosomes which accumulate at the perinuclear and basal surface of the syncytiotrophoblast, the formation of larger autophagosomes which are associated with oxidised lipid, and there is increased expression of the enzyme AOX1. The same changes are observed in placentas associated with stillbirth. Some of our results are semi-quantitative as this is the nature of western analysis, nevertheless the robustness of our results is supported by the use of multiple end points for aging, and the biological plausibility of the reported links. Further supporting our hypothesis, similar changes in oxidation of lipid, localisation of lysosomes and size of autophagosomes occurred

in placental explants deprived of growth factors, and these changes were blocked by inhibition of AOX1.

Stillbirth occurs in approximately 1 in 200 pregnancies in developed countries¹. The Lancet¹ and the BMJ²⁴ have recently highlighted gaps in our knowledge of this condition. Stillbirth frequently occurs in the setting of fetal growth restriction and in this setting telomere shortening and oxidative damage have been observed in associated placentas²⁵. The risk of stillbirth per 1000 continuing pregnancies rises dramatically after 38 weeks of gestation. We have suggested⁴ that stillbirths in late gestation are a consequence of placental aging. More than 90% of pregnancies have delivered by the end of the 40th week of gestation¹⁰, consequently changes that occur in the placenta in pregnancies that have gone past the usual term have little effect on population level infant survival, since most have already delivered. Such late gestation changes may exist in a kind of Medawar's Shadow²⁶ that allows deleterious genes to persist in the population if their damaging effects occur after reproduction, especially if the same genes exert positive actions earlier in pregnancy. This Medawar's Shadow effect has been proposed to explain the high prevalence of Huntington's disease that is associated with increased fertility in early life but disastrous neurological deterioration after reproduction has occurred²⁷. Our immunofluorescence data show high levels of 8OHdG and 4HNE in late-term and stillbirth placentas supporting this postulated pathway to placental aging. Increases in oxidative damages to DNA and lipid have also been reported in Alzheimer's disease^{17, 28}.

We have also seen marked accumulation of particles positive for the lysosomal marker LAMP2 in the perinuclear and basal side of the syncytiotrophoblast of late-term placentas and placentas associated with stillbirth. This phenomenon closely resembles 'lysosomal

positioning' which occurs in cells under nutritional stress²⁹. Autophagy is an important cellular recycling process that involves fusion of acidic lysosomes with the autophagosomes. Our data show that stillbirth and late-term placentas contain larger autophagosomes than 37-39 week placentas indicating inhibition of the autophagic process in these placentas. Our data further indicate that the autophagosomes are coated with oxidised lipid in the form of 4HNE which may play a role in the failure of lysosomal-autophagosome fusion. Such disturbances in the function of autophagosomes may lead to the accumulation of abnormal protein and deterioration in the function of the syncytiotrophoblast.

Stillbirth is not restricted to the late-term setting and is known to be associated with cigarette smoking and growth restriction. It seems likely that smoking accelerates aging related pathways. Evidence for this is the finding that telomere length is reduced in the fetuses of women who actively smoke during pregnancy³⁰, and similar changes are to be expected in the placentas of smokers. Down's syndrome is associated with advanced aging or progeria^{31, 32} and also with increased rates of stillbirth^{33, 34}, raising the possibility that accelerated placental aging may play a part in stillbirth related to Down's and some other congenital anomalies. Similarly placental abruption is associated with growth restriction, maternal smoking and stillbirth, and placental aging may play a part in this condition^{35, 36}.

We have used cultured term placental explants to interrogate the pathways leading to the lipid oxidation and disturbed autophagosome function. We measured production of 4HNE and the diameter of autophagosomes following serum depletion. We observed a significant increase in 4HNE and a significant increase in autophagosome size suggesting inhibition of autophagy by oxidative damage as we had previously observed in the stillbirth and late-term placentas. Raloxifene a potent inhibitor of AOX1 has been shown to reduce oxidative damage in

endothelial cells³⁷. We have demonstrated that the AOX1 inhibitor raloxifene is also able to block the oxidative damage to the lipid in placental explants. The role of AOX1 was confirmed using the GPER1 agonist G1 that has been shown to block AOX1 activation and reduce 4HNE in renal tissue²³. The G1 also blocked the changes in lysosomal positioning within the explants. We report the novel finding of the presence of the cell surface estrogen receptor GPER1 on the syncytiotrophoblast apical membrane, suggesting that this receptor may play a role in modulating oxidative damage within the placenta. It has been shown that urine from pregnant women carrying a fetus with post-maturity syndrome have lower estrogen:creatinine ratios than women carrying normal foetuses³⁸. These data support the possibility that low estrogen concentrations may lead to loss of the cell surface estrogen receptor (GPER1) mediated inhibition of AOX1 and consequently placental oxidative damage and impaired function.

The changes in the late-term placenta occur as the fetus continues to grow and to require additional supplies of nutrients. Post-maturity syndrome is a condition seen in post-dates infants who show evidence of late gestation failure of nutrition³⁹. Normal human infants born at term have 12-14% body fat whereas post maturity syndrome is associated with the birth of a baby with severe wrinkling of the skin due to loss of subcutaneous fat. Post-maturity syndrome is rarely seen in modern obstetric practice where delivery is usually effected before 42 weeks of gestation using induction of labour or caesarean section if labour has not occurred spontaneously. While none of the infants born to mothers in our study exhibited post-maturity syndrome, our data suggest that the physiological function of the placenta after 41 completed weeks is showing evidence of decline that has many features in common with aging in other tissues. The known exponential increase in unexplained intrauterine death that occurs after 38 weeks of gestation may therefore be a consequence of aging of the placenta

and decreasing ability to adequately supply the increasing needs of the growing fetus. This knowledge may impact on obstetric practice to ensure infants are born before the placenta ages to the point of critical failure⁴⁰. However, it is notable that not all placentas in our late-term cohort exhibited evidence of aging and it is known that infants born later in gestation have lower rates of special school needs, with those born at 41 weeks having the lowest rates⁴¹. The conflicting pressures of late gestation increases in stillbirth and falling rates of intellectual disability make obstetric care at this time very challenging, diagnostics that can predict pregnancies at increased risk of stillbirth would be useful and some progress in their development has been made⁴². Our data also indicate that the placenta may provide a tractable model of aging in a human tissue that uniquely ages in a 9 month period of time. The results suggest that the rate of aging of the placenta varies in different pregnancies and raises the possibility that the rate of aging of the placenta may parallel the rate of aging of the associated fetus carrying the same genome. Our work identifies potential therapeutic targets such as AOX1, that may arrest the oxidative damage to placentas in pregnancies identified at high risk of stillbirth when extreme prematurity precludes delivery. Finally, our data raise the possibility that markers of placental oxidative damage and AOX1 mRNA may be released into maternal blood where they may have diagnostic value in predicting the fetus at risk for stillbirth.

Acknowledgements:

The authors would like to thank Mrs. Anne Wright (midwife), all nurses, doctors of John Hunter Hospital, Australia for helping in collection of placental tissues and especially the women who donated their tissues. The authors acknowledge the contribution of Dr Carolyn Mitchell for providing cDNA for amnion, chorion and decidua.

Author Contributions:

K.M. developed the biochemical concept of the project, designed and performed experiments, and analysed the data. Z.S. designed and performed the *in vitro* culture experiments and analysed the data. R.S. developed the clinical concept of the project. J.A. was involved in developing the biochemical concepts of the study. J.M., F.P. and B.A. were involved in the clinical aspects of the project. S.R. was involved in determining the level of mRNA for GPER1 in gestational tissues. The manuscript was written by K.M., R.S. and Z.S. and approved by all authors.

Footnote: * Figure 1 reprinted from “Smith R, Maiti K, Aitken R. Unexplained antepartum stillbirth: A consequence of placental aging? Placenta 2013;34:310-13” with permission from Elsevier.

References

1. Flenady V, Middleton P, Smith GC, et al. Stillbirths: The way forward in high-income countries. *Lancet* 2011;377:1703-17.
2. Sutan R, Campbell D, Prescott G, Smith W. The risk factors for unexplained antepartum stillbirths in scotland, 1994 to 2003. *J Perinatol* 2010;30:311-18.
3. Johnson FB, Sinclair DA, Guarente L. Molecular biology of aging. *Cell* 1999;96:291-302.
4. Smith R, Maiti K, Aitken R. Unexplained antepartum stillbirth: A consequence of placental aging? *Placenta* 2013;34:310-13.
5. Amir H, Weintraub A, Aricha-Tamir B, Apel-Sarid L, Holcberg G, Sheiner E. A piece in the puzzle of intrauterine fetal death: Pathological findings in placentas from term and preterm intrauterine fetal death pregnancies. *J Matern Fetal Neonatal Med* 2009;22:759-64.
6. Labarrere CA, Dicarlo HL, Bammerlin E, et al. Failure of physiologic transformation of spiral arteries, endothelial and trophoblast cell activation, and acute atherosclerosis in the basal plate of the placenta. *Am J Obstet Gynecol* 2017;216:287 e1-87 e16.
7. Ferrari F, Facchinetti F, Saade G, Menon R. Placental telomere shortening in stillbirth: A sign of premature senescence? *T J Matern Fetal Neonatal Med* 2016;29:1283-88.
8. Biron-Shental T, Sukenik-Halevy R, Sharon Y, et al. Short telomeres may play a role in placental dysfunction in preeclampsia and intrauterine growth restriction. *Am J Obstet Gynecol* 2010;202:381 e1-7.
9. Maiti K, Paul J, Read M, et al. G-1-activated membrane estrogen receptors mediate increased contractility of the human myometrium. *Endocrinology* 2011;152:2448-55.
10. Omigbodun AO, Adewuyi A. Duration of human singleton pregnancies in ibadan, nigeria. *J Natl Med Assoc* 1997;89:617.
11. Hirano T, Yamaguchi R, Asami S, Iwamoto N, Kasai H. 8-hydroxyguanine levels in nuclear DNA and its repair activity in rat organs associated with age. *J Gerontol A Biol Sci Med Sci* 1996;51:B303-7.
12. Lovell MA, Markesbery WR. Oxidative DNA damage in mild cognitive impairment and late-stage alzheimer's disease. *Nucleic Acids Res* 2007;35:7497-504.
13. Hardy J, Selkoe DJ. The amyloid hypothesis of alzheimer's disease: Progress and problems on the road to therapeutics. *Science* 2002;297:353-56.

- 475 14. Goedert M, Spillantini M, Jakes R, Rutherford D, Crowther R. Multiple isoforms of
476 human microtubule-associated protein tau: Sequences and localization in
477 neurofibrillary tangles of alzheimer's disease. *Neuron* 1989;3:519-26.
- 478 15. Carter RJ, Lione LA, Humby T, et al. Characterization of progressive motor deficits in
479 mice transgenic for the human huntington's disease mutation. *J Neurosci*
480 1999;19:3248-57.
- 481 16. Erie C, Sacino M, Houle L, Lu ML, Wei J. Altered lysosomal positioning affects
482 lysosomal functions in a cellular model of huntington's disease. *Eur J Neurosci*
483 2015;42:1941-51.
- 484 17. Markesbery W, Lovell M. Four-hydroxynonenal, a product of lipid peroxidation, is
485 increased in the brain in alzheimer's disease. *Neurobiol Aging* 1998;19:33-36.
- 486 18. Boland B, Kumar A, Lee S, et al. Autophagy induction and autophagosome clearance
487 in neurons: Relationship to autophagic pathology in alzheimer's disease. *J Neurosci*
488 2008;28:6926-37.
- 489 19. Tanaka Y, Guhde G, Suter A, et al. Accumulation of autophagic vacuoles and
490 cardiomyopathy in lamp-2-deficient mice. *Nature* 2000;406:902-06.
- 491 20. Lee J-A, Beigneux A, Ahmad ST, Young SG, Gao F-B. Escrt-iii dysfunction causes
492 autophagosome accumulation and neurodegeneration. *Curr Biol* 2007;17:1561-67.
- 493 21. Garattini E, Terao M. Increasing recognition of the importance of aldehyde oxidase in
494 drug development and discovery. *Drug Metab Rev* 2011;43:374-86.
- 495 22. Obach RS. Potent inhibition of human liver aldehyde oxidase by raloxifene. *Drug*
496 *Metab Dispos* 2004;32:89-97.
- 497 23. Lindsey SH, Yamaleyeva LM, Brosnihan KB, Gallagher PE, Chappell MC. Estrogen
498 receptor gpr30 reduces oxidative stress and proteinuria in the salt-sensitive female
499 mren2.Lewis rat. *Hypertension* 2011;58:665-71.
- 500 24. Gardosi J, Madurasinghe V, Williams M, Malik A, Francis A. Maternal and fetal risk
501 factors for stillbirth: Population based study. *BMJ* 2013;346:f108.
- 502 25. Davy P, Nagata M, Bullard P, Fogelson N, Allsopp R. Fetal growth restriction is
503 associated with accelerated telomere shortening and increased expression of cell
504 senescence markers in the placenta. *Placenta* 2009;30:539-42.
- 505 26. Medawar PB. *An unsolved problem of biology*. University College, London; 1952.

27. Eskenazi BR, Wilson-Rich NS, Starks PT. A darwinian approach to huntington's disease: Subtle health benefits of a neurological disorder. *Med Hypotheses* 2007;69:1183-89.
28. Lovell MA, Gabbita SP, Markesbery WR. Increased DNA oxidation and decreased levels of repair products in alzheimer's disease ventricular csf. *J Neurochem* 1999;72:771-76.
29. Korolchuk VI, Saiki S, Lichtenberg M, et al. Lysosomal positioning coordinates cellular nutrient responses. *Nat Cell Biol* 2011;13:453-60.
30. Salihu HM, Pradhan A, King L, et al. Impact of intrauterine tobacco exposure on fetal telomere length. *Am J Obstet Gynecol* 2015;212:205.e1-8.
31. Adorno M, Sikandar S, Mitra SS, et al. Usp16 contributes to somatic stem-cell defects in down's syndrome. *Nature* 2013;501:380-4.
32. Souroullas GP, Sharpless NE. Stem cells: Down's syndrome link to ageing. *Nature* 2013;501:325-26.
33. Morris JK, Wald NJ, Watt HC. Fetal loss in down syndrome pregnancies. *Prenat Diagn* 1999;19:142-5.
34. Frey HA, Odibo AO, Dicke JM, Shanks AL, Macones GA, Cahill AG. Stillbirth risk among fetuses with ultrasound-detected isolated congenital anomalies. *Obstet Gynecol* 2014;124:91-8.
35. Ananth CV, Williams MA. Placental abruption and placental weight - implications for fetal growth. *Acta Obstet Gynecol Scand* 2013;92:1143-50.
36. Matsuda Y, Hayashi K, Shiozaki A, Kawamichi Y, Satoh S, Saito S. Comparison of risk factors for placental abruption and placenta previa: Case-cohort study. *J Obstet Gynaecol Res* 2011;37:538-46.
37. Wassmann S, Laufs U, Stamenkovic D, et al. Raloxifene improves endothelial dysfunction in hypertension by reduced oxidative stress and enhanced nitric oxide production. *Circulation* 2002;105:2083-91.
38. Rayburn WF, Motley ME, Stempel LE, Gendreau RM. Antepartum prediction of the postmature infant. *Obstet Gynecol* 1982;60:148-53.
39. Moya F, Grannum P, Pinto K, Bracken M, Kadar N, Hobbins JC. Ultrasound assessment of the postmature pregnancy. *Obstet Gynecol* 1985;65:319-22.
40. Nicholson JM, Kellar LC, Ahmad S, et al. US term stillbirth rates and the 39-week rule: A cause for concern? *Am J Obstet Gynecol* 2016;214:621.e1-9.

41. Mackay DF, Smith GC, Dobbie R, Pell JP. Gestational age at delivery and special educational need: Retrospective cohort study of 407,503 schoolchildren. *PLoS Med* 2010;7:e1000289.
42. Chaiworapongsa T, Romero R, Korzeniewski SJ, et al. Maternal plasma concentrations of angiogenic/anti-angiogenic factors in the third trimester of pregnancy to identify the patient at risk for stillbirth at or near term and severe late preeclampsia. *Am J Obstet Gynecol* 2013;208:287.e1-87.e15.

List of Tables and Figures

Table 1: Demographic and clinical characteristics of the study subjects.

Figure Legends:

Figure 1: Relationship between stillbirth and number of continuing pregnancies. Kaplan Myer plot of number of continuing pregnancies as a function of gestational age and plot of unexplained stillbirth per 1000 continuing pregnancies, data from Omigbodun and Adewuyi¹⁰ and Sutan et al.². Plot shows the increase in risk of stillbirth with time consistent with the operational definition of aging proposed by Johnson et al.³ and the relatively small number of pregnancies at risk of stillbirth by 41 weeks because of prior delivery. Reproduced with permission from Smith et al.,^{4*}

Figure 2: DNA/RNA oxidation in late-term and stillbirth placentas. Confocal microscopy showed increased 8OHdG staining (red) in nuclei from late-term (B) and stillbirth placentas (C) compared to 37-39 week placentas (A). DAPI (blue) staining identifies the nuclei. The graph (D) illustrates that late-term and stillbirth placentas have increased intensity of nuclear 8OHdG staining ($p < 0.0001$ for late-term placentas, $p = 0.0005$ for stillbirth placentas, Mann Whitney test) compared to 37-39 week placentas. In Figure 2D open circles and filled circles represent 37-39 week caesarean non-labouring placentas ($n=10$) and vaginal delivery labouring placentas ($n=8$) respectively, and open squares and filled squares represent late-term labouring caesarean placentas ($n=5$) and labouring vaginal delivery placentas ($n=13$) respectively, and filled triangles represent third trimester labouring vaginal delivery unexplained stillbirth placentas ($n=4$). Each point in the graph represents the average intensity

of 8OHdG of 60 nuclei in 6 images per placenta photographed at 100X magnification and 1.4 optical resolution. Scale bar, 20 μ m. The microscopy also indicates increased staining in the cytosol of late-term and stillbirth placentas representing oxidised RNA (8-hydroxyguanosine) that is also detected by the antibody.

Figure 3: Changes in lysosomal distribution in late-term and stillbirth placentas. IHC of LAMP2 (red), a lysosomal marker showed that lysosomes predominantly localise to the apical surface of 37-39 week placentas (A), whereas lysosome distribution extends to the perinuclear and basal surface of syncytiotrophoblast in late-term (B) and stillbirth placentas (C). Intensity calculation across the syncytiotrophoblast showed that the distribution of LAMP2 in late-term (n=5, Figure 3F) and unexplained stillbirth placentas (n=4, Figure 3G) shifts to the perinuclear and basal surface whereas lysosome distribution in 37-39 week caesarean placentas (n=5, Figure 3D) and vaginal delivery placentas (n=5, Figure 3E) remained in the apical region of the syncytiotrophoblast. DAPI (blue) staining identifies the nuclei. In Figures 3D to 3G each coloured line represents results on an individual placenta, and shows the mean intensity of LAMP2 across the syncytiotrophoblast at 5 random sites per image (example represented by light green line in 3A, 3B and 3C) for 6 separate images per placenta. Images were photographed at 100X magnification; scale bar, 20 μ m.

Figure 4: Lipid peroxidation is increased in late-term and stillbirth placentas. 4HNE (red) immunostaining in 37-39 week (A), late-term (B), and stillbirth (C) placentas. DAPI (blue) staining identifies nuclei. The intensity of 4HNE is significantly increased in late-term placentas (D) ($p<0.0001$, Mann Whitney test) and stillbirth placentas ($p=0.0014$, Mann Whitney test). In Figure 4D open circles and filled circles represent 37-39 week caesarean non-labouring placentas (n=20) and vaginal delivery labouring placentas (n=14) respectively,

and open squares and filled squares represent late-term labouring caesarean placentas (n=10) and vaginal delivery placentas (n=18) respectively, while filled triangles represent third trimester labouring vaginal delivery unexplained stillbirth placentas (n=4). Each point in 4D represents the mean intensity per unit area for 6 images taken for each individual placenta. Images were photographed at 100X magnification; scale bar, 20 μ m.

Figure 5: Larger autophagosomes occur in late-term and stillbirth placentas.

Immunofluorescence staining of LC3B (green) in the 37-39 week (A), late-term (B), and unexplained stillbirth (C) placentas. DAPI (blue) staining indicates the nuclei. Autophagosome size was quantified using NIS element software and the diameter was measured at an arbitrary intensity range of 1000-3000, diameter range 0.2-1 μ m and circularity range 0.5-1. Analysis (D) showed that late-term and stillbirth placentas have significantly larger (p=0.012 and p=0.0019, respectively, Mann Whitney test) autophagosomes than 37-39 week placentas. In 'D' open circles and filled circles represent 37-39 week caesarean non-labouring placentas (n=11) and vaginal delivery labouring placentas (n=10) respectively, and open squares and filled squares represent late-term labouring caesarean placentas (n=8) and labouring vaginal delivery placentas (n=15) respectively, while filled triangles represents unexplained stillbirth placentas (n=4). Each point in the graph represents the average diameter of LC3B particles in six images taken for each placenta. Original magnification, 100X; scale bar, 20 μ m. Arrow heads indicate autophagosomes (LC3B positive particles).

Figure 6: Co-localisation of aldehyde oxidase (AOX1) and 4HNE, and increased expression of AOX1 mRNA in late-term and stillbirth placentas. Representative dual labelled fluorescence immunostaining in late-term (A-C) and stillbirth (D-F) placentas

showed that AOX1 positive particles (green) are co-localized with 4HNE (red). Orange dots (pointed by arrow heads in C and F) indicate co-localization. Nuclei are stained with DAPI (blue). Real-time PCR showed that expression of AOX1 mRNA is increased in late-term (p=0.0097) and stillbirth (p=0.012) placentas compared to early-term placentas (G). Original magnification 100X; scale bar 20 μ m.

Figure 7: Pharmacologic inhibition of 4HNE production. Fluorescence immunostaining with antibody against 4HNE (red) in serum starved placental explant (A) at time 0 (just before starvation) (B) at 24 h after culturing in medium containing FBS (control treatment), (C) at 24 after starvation (culturing in medium without FBS), (D) 24 h after treatment with an AOX1 inhibitor, raloxifene (RLX) and (E) 24 h after treatment with a membrane estrogen receptor GPER1 agonist, G1. Intensity calculation showed that the production of 4HNE (induced by serum starvation) is significantly reduced after treating placental explants with raloxifene (F) and G1 (G). Data are mean \pm S.E.M., * p <0.05 (N=6). Original magnification, 20X; scale bar, 100 μ m. DAPI (blue) staining indicates the nuclei.

Figure 8: Expression of GPER1 in placenta and myometrium, but not in membranes by IHC, real-time PCR and western-blotting. Fluorescence IHC showed that GPER1 (green) is localized predominantly in the placental in a section of a term placental roll photographed at 10X magnification (A). GPER1 (green) was shown to localize in the apical layer of syncytiotrophoblast of placental villi (B), when photographed at 100X magnification. Scale bar in 'A' and 'B' represent 100 μ m and 20 μ m, respectively. The real-time qPCR data showed that the mRNA for GPER1 is expressed in higher amounts in term placenta, whereas amnion, chorion and decidua show very low expression of GPER1 (C). The expression of mRNA for GPER1 follows the order: decidua<chorion<amnion<placenta. The western blot of

protein extract from the breast cancer cell line MCF-7, term placenta, myometrium, amnion, chorion and decidua are presented in 'D'. Placenta, myometrium and MCF-7 cell lines expressed higher amounts of GPER1 than amnion, chorion or decidua (D). Western-blotting data showed that all the tissues expressed glycosylated GPER1 (denoted by ** or by ***) and non-glycosylated nascent GPER1 (denoted by *). The sypro-ruby stain of the same PVDF membrane is used as internal loading control (E).

Supplementary Figure Legends

Figure S1: Oxidised lipids within autophagosomes of late-term placentas. Representative dual labelled fluorescence immunostaining showed that LC3B, an autophagosome marker (green) is co-localised with 4HNE, a marker of lipid peroxidation (red). Orange dots (pointed by arrow heads in C) indicate the co-localization. DAPI (blue) staining indicates the nuclei. Original magnifications 100X; scale bar 20 μ m.

Figure S2: Changes in autophagosome size in placental explants cultured in serum deprived medium. Fluorescence immunostaining with antibody against LC3B (green) in serum starved placental explant (A) at time 0 (just before starvation) and (B) at 24 h after starvation. DAPI (blue) staining indicates nuclei. (C) Immunohistochemical analysis showed that the size of autophagosomes (LC3B positive particles) increased 24 h after serum starvation compared to 0 h. Data presented as mean \pm S.E.M., ***p=0.0002 (N=13). Scale bar, 20 μ m.

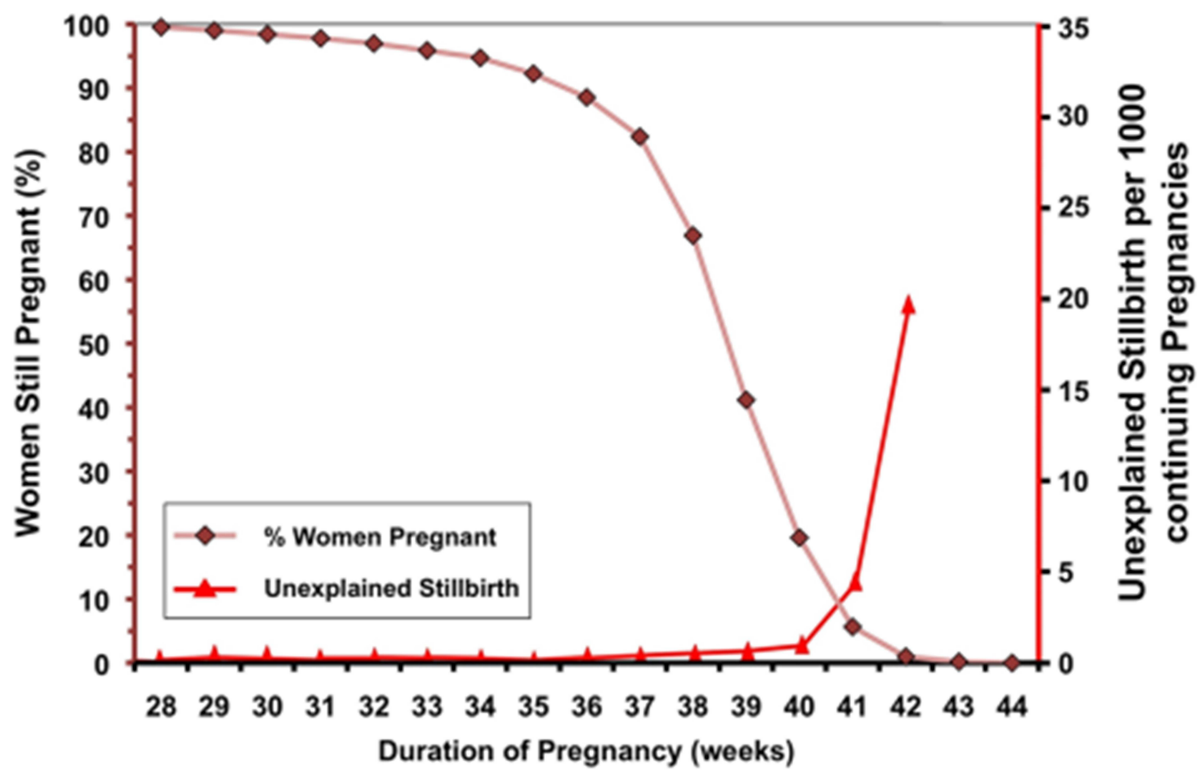
Figure S3: GPER1 regulates lysosomal distribution in placental explants cultured in serum deprived medium. Fluorescence immunostaining with antibody against LAMP2

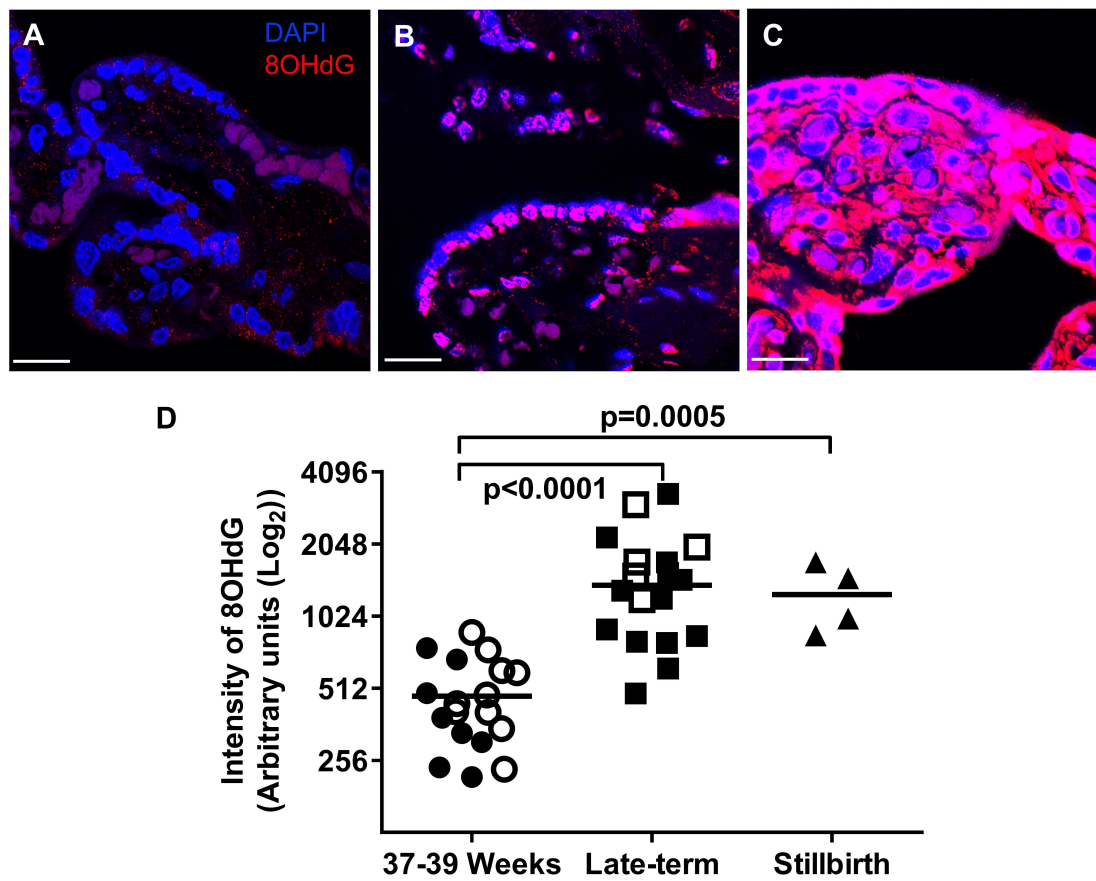
672 (red) in serum starved placental explant (A) at time 0 (just before starvation), (B) at 24 h after
673 culturing in medium containing FBS, (C) at 24 h after starvation (culturing in medium without)
674 FBS, and (D) 24 h after treatment with GPER agonist, G1. DAPI (blue) staining indicates
675 nuclei. Intensity calculation (E) across the syncytiotrophoblast showed that the distribution of
676 LAMP2 at 24 h after starvation shifts to the perinuclear and basal surface compared to control
677 treatment (N=7). Each coloured line in 'E' represents the mean intensity of LAMP2 across the
678 syncytiotrophoblast at 5 random sites per image for 6 separate images per experiment. In 'F',
679 each coloured bar indicates mean of the area under the curve (AUC) of the corresponding
680 coloured line presented in 'E' and statistical differences were calculated. Original
681 magnifications, 40X; scale bar, 20 μ m; error bar, S.E.M.; * $p < 0.05$ (N=7).

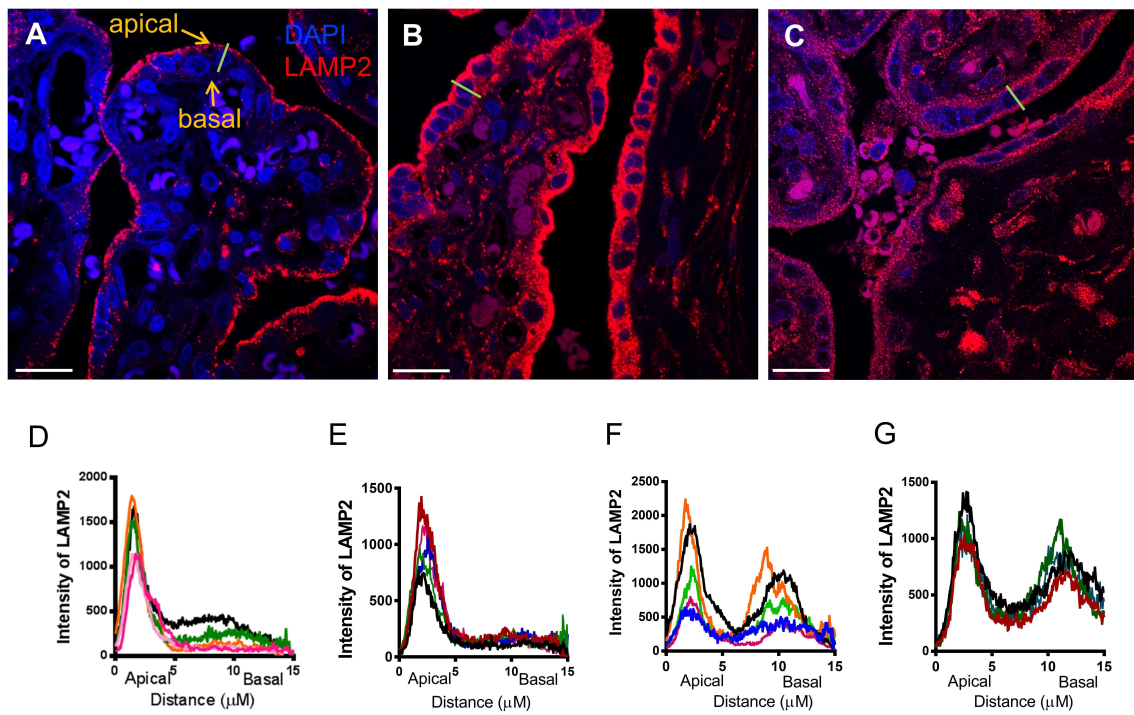
Table 1: Demographic and clinical characteristics of the study subjects

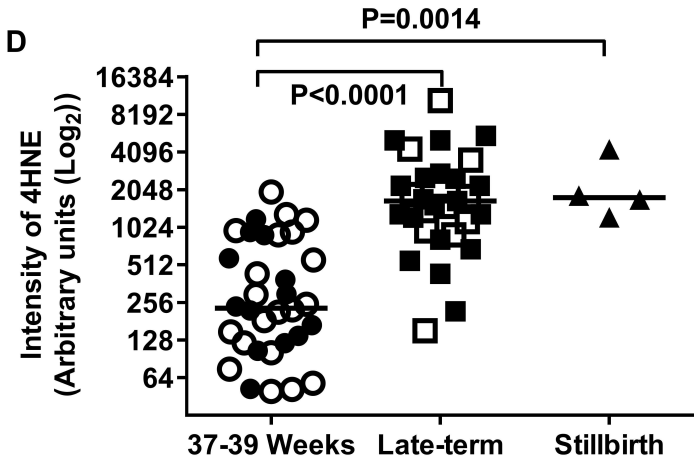
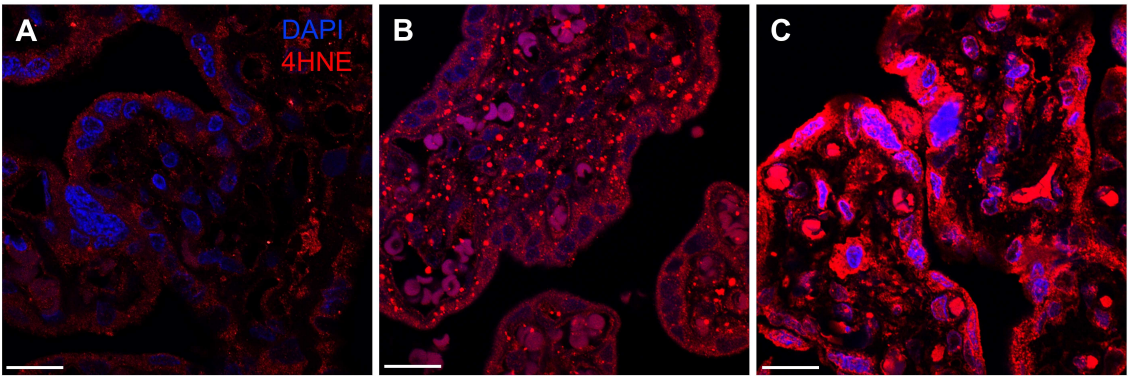
Characteristic	37-39 Weeks	Late-term	Stillbirth			
Number of cases	34	28	4			
Gestational ages (weeks)	38.57 \pm 0.15	41.46 \pm 0.06	32	32.57	39	40.14
Fetal growth restriction (number of cases)	0	0	No	Yes	No	Yes
Maternal age (years)	31.03 \pm 0.88	28.81 \pm 1.15	30.21 \pm 2.68			
Vaginal birth (%)	41.20 %	64.30 %	100.00 %			
BMI (kg/m ²) at second trimester or at birth	29.10 \pm 1.50	28.52 \pm 1.10	27.40 \pm 2.40			
Ethnicity						
Caucasian (%)	82.35 %	96.42 %	75.00 %			
Smoker (%)	17.64 %	17.85 %	0.00 %			

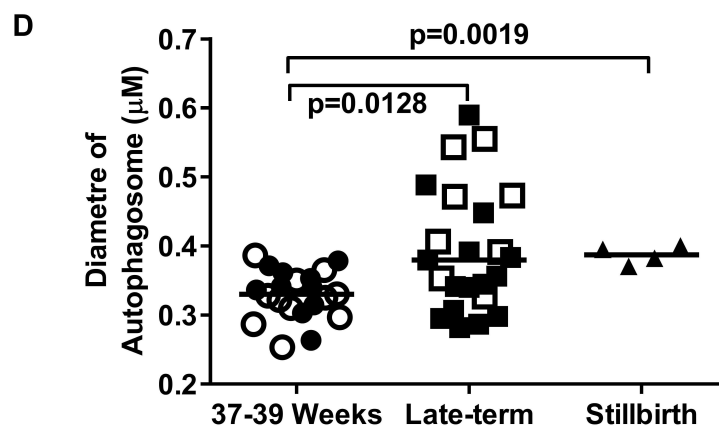
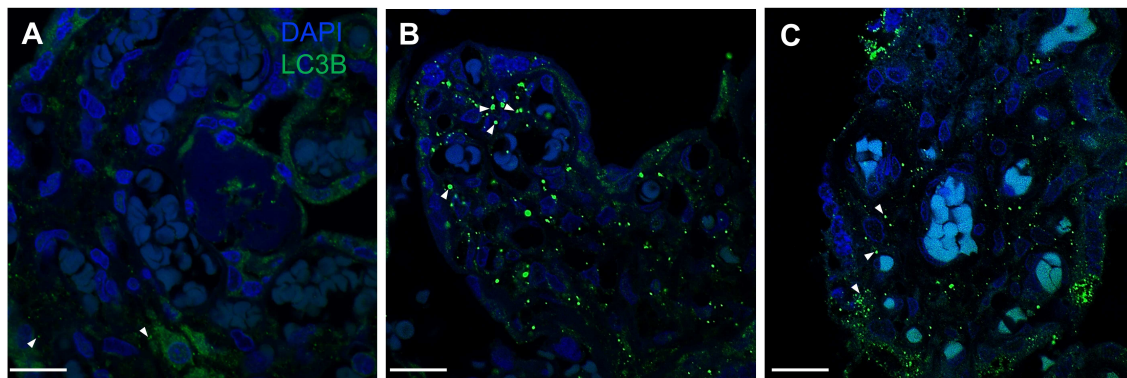
Data are presented as (Mean \pm SEM) or percentage. BMI, Body Mass Index

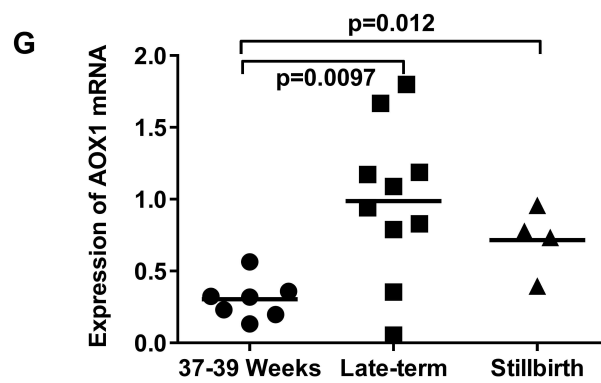
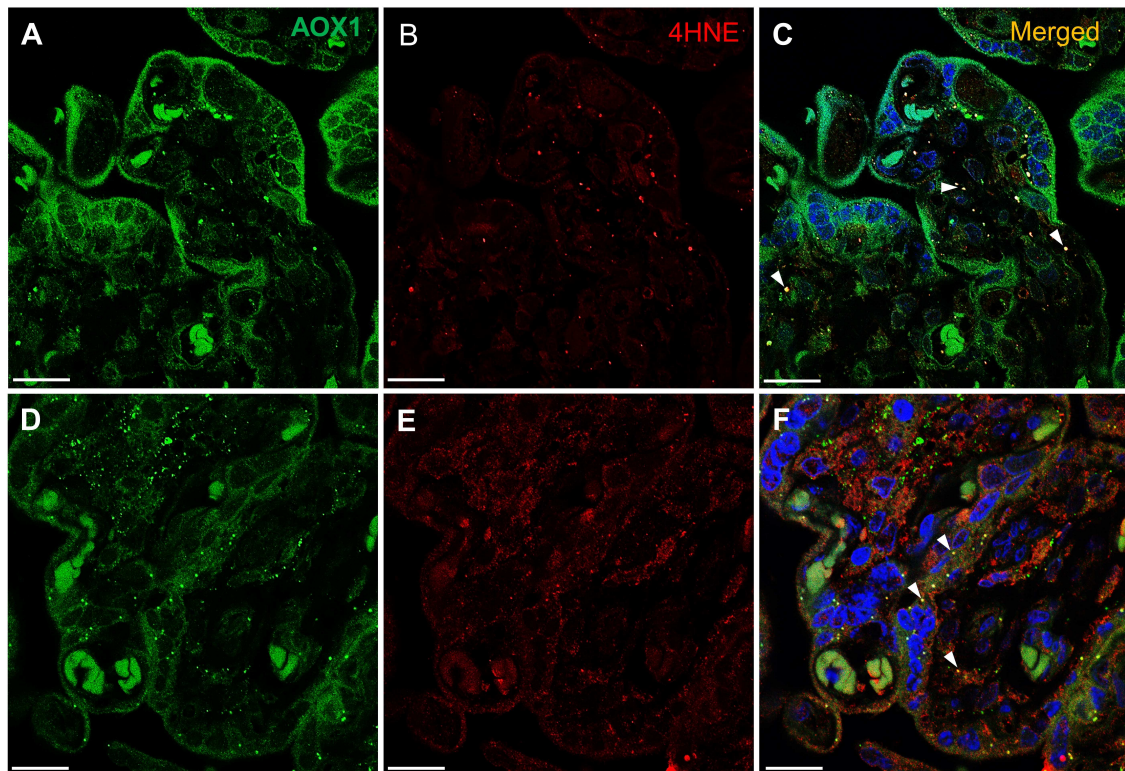


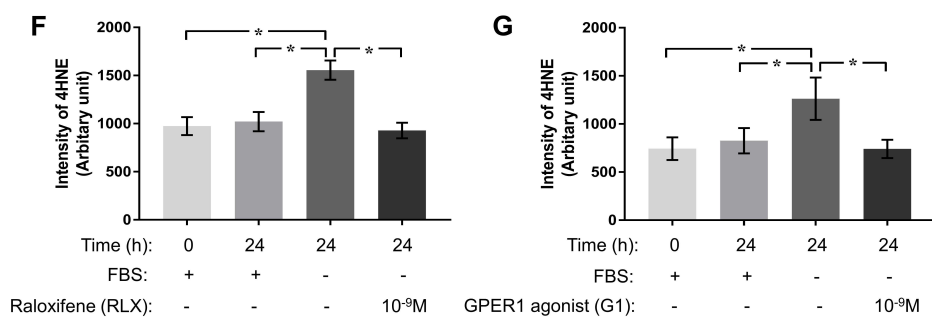
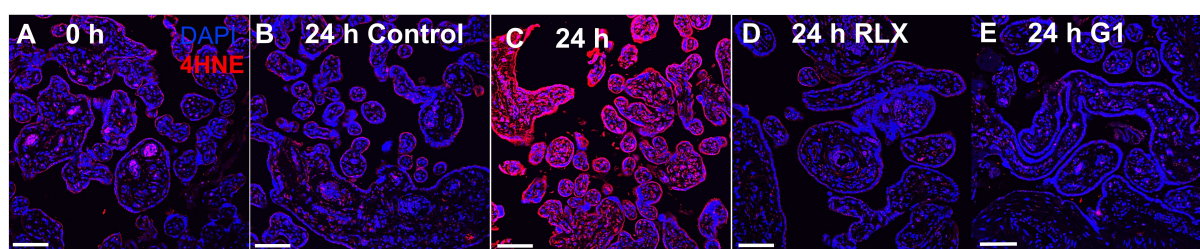


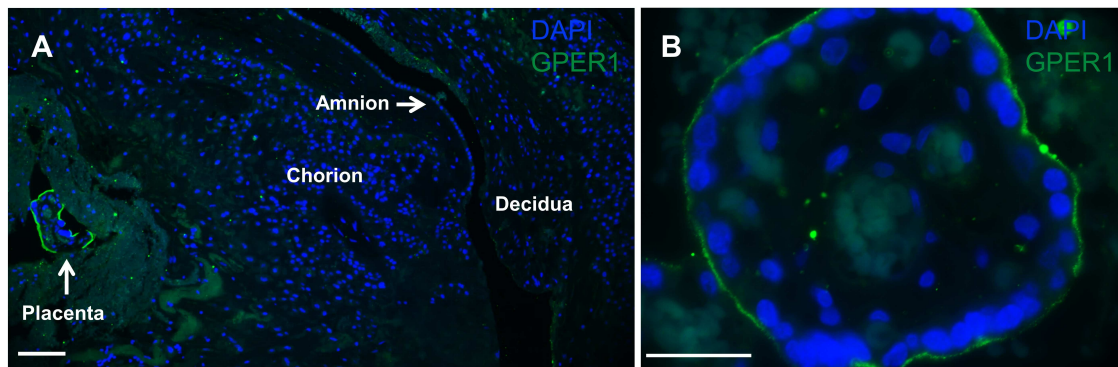




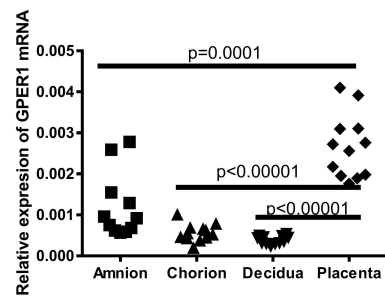




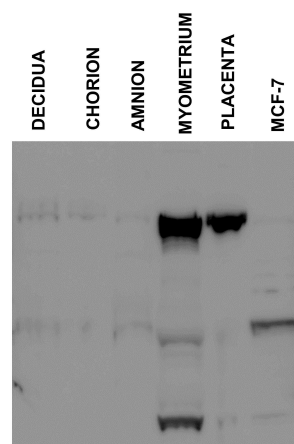




C



D



E

